



RESEARCH ARTICLE

Channel Estimation Enhancement in Cell-Free Massive MIMO Systems under Pilot Contamination

Mohammed Dawood Alrubay^{1*}, Hayder Almosa²¹Department of Electrical Engineering, Faculty of Engineering, University of Kufa, Najaf, Iraq² Department of Electronic and Communication Engineering, University of Kufa, Najaf, Iraq

ARTICLE INFO	ABSTRACT
Received: May 25, 2024 Accepted: Jun 27, 2024	In this scholarly context, we delve into the realm of cell-free massive Multiple-Input Multiple-Output (MIMO) systems. These systems feature a multitude of single-antenna, low-cost, and low-power access points distributed across the coverage area. These access points are seamlessly connected to a central network controller. Notably, cell-free massive MIMO operates without the traditional constraints of cellular boundaries. Our research endeavors focus on enhancing the efficiency of cell-free massive MIMO systems. To this end, we propose a novel pilot decontamination algorithm that mitigates pilot contamination during channel estimation. This algorithm aims to address the challenge of pilot contamination, which arises when the available pilot resources are insufficient to serve all users effectively. Our approach involves judiciously sharing pilot resources among multiple users and employing dedicated algorithms in the pilot contamination domain to separate their signals. In conventional cell-free massive MIMO setups, users typically utilize unique orthogonal training signals. However, this necessitates a substantial pool of such sequences. Alternatively, in scenarios where there is a scarcity of training signals, pilot contamination phenomena come into play. Unfortunately, the reuse of pilot training signals introduces user interference due to shared resources. To mitigate this challenge and enhance the quality of channel estimation, we propose a combined approach that leverages both Principal Component Analysis (PCA) and the Least Mean Squares (LMS) algorithms. Specifically, we implement this approach for user separation within the shared pilot sequence. Our results demonstrate that this method significantly reduce the pilot contamination effect and improves the performance in compared to traditional method used.
Keywords Cell-free massive MIMO Pilot contamination Channel estimation System efficiency	
*Corresponding Author: mohammed.alrubay@ student.uokufa.edu.iq	

INTRODUCTION

Cell-free massive MIMO architectures, wherein a plethora of single-antenna access points (APs) concurrently cater to a relatively smaller user base within the network utilizing identical frequency resources, have garnered considerable interest. This is attributed to their ability to deliver consistently high-quality service across all users and obviate the necessity for handover [1] [2] [3] [4]. Furthermore, the integration of multiple-antennas at APs bestows upon cell free massive MIMO the crucial advantage of channel hardening, a characteristic also inherent to massive MIMO systems [5] [6] [7] [8]. In the context of Cell-Free Massive MIMO systems, two pivotal parameters significantly

impact system performance: pre-coders and power allocation algorithms. These parameters play a crucial role in optimizing comprehensive efficacy and performance metrics of the system are under consideration [9]. The concept of multi-cell Massive MIMO configurations, characterized by each cellular division being equipped with an associated array of antennas, is widely recognized in the field [10] [11] [12] [13]. However, an alternative The implementation of Massive MIMO technology is designed to provide uniform coverage across a designated region, which may encompass a remote hamlet, an academic institution's grounds, or a metropolitan expanse, via a dispersed network of access stations with a single antenna access points situated at random intervals. In the context of massive Multiple-Input Multiple-Output (MIMO) systems, effective pilot assignment plays a pivotal role in mitigating inter-cell interference and enhancing uplink performance. Our proposed Smart Pilot Assignment (SPA) scheme strategically allocates pilot sequences to users depending on the interference levels that are present and their channel quality. By prioritizing users with weaker channels and minimizing inter-cell interference, SPA significantly improves the minimum uplink Signal-to-Interference-Plus-Noise Ratio (SINR) for all users within the target cell. Theoretical analysis further substantiates that SPA approaches the optimal solution, particularly as the number of base station antennas increases. This underscores the importance of intelligent pilot assignment strategies in realizing the full potential of massive MIMO system [14].

Figure 1 presents a comparative analysis of multi-cell MIMO systems versus cell free massive MIMO configurations. Multi cell MIMO systems employ multiple base stations, each equipped with either a single antenna or a limited number of antennas. These base stations serve specific designated areas, effectively creating multiple cells. Users connect to the base station with the strongest signal, but interference may arise between users at the edges of different cells. In contrast, cell-free massive MIMO utilizes a large number of antennas distributed across a coverage area. Notably, there is no concept of individual cells; instead, all antennas collaborate coherently to serve users. Users receive service from a collective signal generated by multiple antennas, leading to reduced interference and improved coverage. In essence, cell-free massive MIMO represents a more flexible and potentially more efficient approach compared to traditional multi-cell MIMO systems.

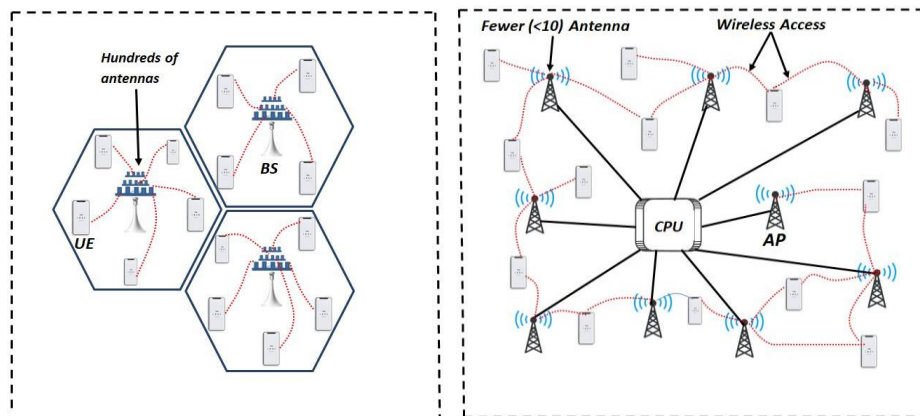


Figure 1: comparison between multi-cell MIMO and cell-free massive MIMO

This system is called Cell Free Massive MIMO [15]. Addressed the significant interference issues in current cellular networks, which arise from the autonomous operation of cells. The objective was to establish a scalable framework for Cell-Free Massive MIMO systems, utilizing the dynamic cooperation cluster principle derived from Network MIMO studies. The scholars introduced an innovative algorithm that integrates initial access, pilot assignment, and cluster creation, all structured to promote scalability. They also adapted standard methods for channel estimation, precoding, and combining to fit this scalable framework. Additionally, they proved a new uplink and downlink duality, using it to design precoding vectors based on combining vectors. Numerical evaluations showed that the proposed scalable framework achieved performance close compared to

cutting-edge unscalable methods and far exceeded the initial Cell-Free Massive MIMO algorithms based on maximum ratio (MR)[16]. The researchers proposed a brand-new cluster formation, pilot assignment, and initial access algorithm, designed to ensure scalability. They also adapted standard methods for channel estimation, precoding, and combining to fit this scalable framework. Additionally, they proved a new uplink and downlink duality, using it to design precoding vectors based on combining vectors. Within cell-free systems, the entirety of channel estimations ascertained the pilot signals employed to precode data during the transmission in the downlink and making decoding during the transmission in the uplink. During the phase first training, it is optimal for each user to receive a distinct pilot sequence that maintains orthogonality with the pilot sequences allocated to other users. Nevertheless, this becomes challenging when the coherence interval is brief and/or the user population within the system is substantial [17] [18], users have to use non-orthogonal pilot sequences, the consequence is that at each access point (AP), the pilot signal emitted by an individual user incurs interference from the pilot signals of other users. This phenomenon, termed pilot contamination, markedly impairs the overall performance of the system [19] [20]. Pilot contamination can be mitigated by using pilot assignment and data power controls [1] [11] [21]. In prior research concerning cell-free massive MIMO systems, it has been customary for all pilot signals to be broadcast at their highest power output throughout the training phase [1] [3] [11] [12]. During the training phase, it may occur that a user possessing suboptimal channel conditions experiences significant interference from users endowed with robust channels. This interference can markedly degrade the individual user's performance, which, in turn, detrimentally impacts the aggregate efficiency of the systems [11] [22].

Non-orthogonal pilots in cell-free massive MIMO systems enable a more optimal pilot resource allocation among many devices, mitigating the pilot contamination problem. Unlike orthogonal pilots, which assign a unique pilot sequence to each device and cause interference among them when the device number is large, non-orthogonal pilots allow multiple devices to use the same pilot sequence and still be identifiable by their channel statistics. This reduces the pilot contamination effect and improves the channel estimation quality and system performance [23] [24].

In the present study, we conduct a comprehensive examination of an extensive cell-free Massive MIMO system as delineated within the scope of this paper [15], where we handle limited pilot signals and use pilot contamination mandated for user utilization. Consequently, this results in a certain user's pilot signal at each Access Point (AP) causing interference with the pilot signals transmitted by other users. Pilot Contamination Mitigation in Cell-Free Massive MIMO Systems. The phenomenon known as pilot contamination significantly impacts the performance of wireless communication systems. To address this challenge, it becomes imperative to separate common channels that share the same pilot signal. In our approach, we employ a combination of Principal Component Analysis (PCA) and the Least Mean Squares (LMS) algorithm to effectively segregate user signals associated with shared pilots. This joint application of PCA and LMS yields improved results, leading to substantial enhancements in system performance.

This paper's subsequent sections are organized like this: System Model (Section 2): We delve into the fundamental aspects of our cell-free massive MIMO system. Channel Estimation (Section 3): Here, we discuss the intricacies of channel estimation techniques. PCA Algorithm and LMS Algorithm (Sections 4, 5): We explore the details of our proposed algorithms for user separation within the shared pilot sequence. Numerical Results and Discussions (Section 6): We present empirical findings and engage in insightful discussions. Conclusion (Section 7): Finally, we summarize our contributions and highlight future research directions.

System Model

We consider a cell-free system where there is no cell division inside the network, but rather consists of a singular expansive cell that is outfitted with N access points, and U users, also each with a single antenna. All access points, which are also called antennas in this paper, serve all users and are interfaced with a network control unit. The antenna's channel coefficient, n and user, u is given by:

$$h_{nu} = \sqrt{\beta_{nu}} g_{nu} \quad (1)$$

Where β_{nu} is the coefficient to large-scale fading that captures the attenuation of signal strength, known as path loss, along with the shadowing effects, are characterized by a coefficient that exhibits gradual variation over time. This coefficient can be systematically observed and predicted with a degree of accuracy. Unlike co-located systems, the cell free system experiences large-scale fading, the large scale fading differs for every user and access point pair. The second element $g_{nu} \sim \mathcal{CN}(0,1)$ is the coefficient small-scale fading. We consider these coefficients to be random variables with equal distributions and independence. Utilizing the block fading model, we make the assumption that g_{nu} ($1 \leq n \leq N, 1 \leq u \leq U$) stays the same during a coherent interval and varies on its own throughout other coherent intervals. Additionally, we make the assumption that the channel coefficients for uplink and downlink broadcasts are the identical, or channel reciprocity. The channel matrix that connects every antenna to every user is shown by $H \in \mathbb{C}^{N \times U}$, with $[H]_{nu} = h_{nu}$.

Channel Estimation

With no cells in a massive MIMO system, we presume $N \geq U$. The transmitter must be aware of the channel state information (CSI) in order to achieve high throughput. Antenna, n must thus calculate the channel coefficients. $h_{nu} \quad u = 1, \dots, U$. The protocol known as time-division duplex can be used for this. As part of this protocol, each user sends a training signal at *initially* $\varphi_1, \dots, \varphi_U$ to the antennas synchronously. The second phase involves estimating the channel coefficients for each antenna and beamforming data to every user using these estimations. There are around (1400) pilots in mutual orthogonality using half of the coherence time if their velocity is less than (10 km/h) and their carrier-frequency is (1.9 GHz). Therefore, it seems sense to presume that users who must repurpose the same training signal will be spread apart from one another and that there won't be much pilot contamination—that is, coherent interference brought on by two or more users using the same pilot sequence. Therefore, we presume that pilot sequences of length that are mutually orthogonal $\tau \geq U$, i.e. $\varphi_i^H \varphi_j = \delta_{ij}$, and we will also use non-orthogonal training signals of length $\geq U$, $\varphi_i^H \varphi_j = \delta_{i \neq j}$, are assigned to users, and we take into consideration the noise-induced channel estimate error directly. In the training phase at antenna, n , the received signal sequence is

$$y_n = \sqrt{\rho_r \tau} \sum_{i=1}^U h_{ni} \varphi_i + s_n \quad (2)$$

Where ρ_r symbolizes the strength of the uplink and $s_n \sim \mathcal{CN}(0, I_\tau)$ is Additive Gaussian Noise (AWGN). The MMSE estimation of h_{nu} is

$$\hat{h}_{nu} = \frac{\sqrt{\rho_r \tau} \beta_{nu}}{1 + \rho_r \tau \beta_{nu}} \varphi_u^H y_n \quad (3)$$

Let $\hat{h}_{nu} = h_{nu} - \hat{h}_{nu}$ be the error in channel estimation. It is commonly recognized that there is no correlation between \hat{h}_{nu} and h_{nu} , and

$$\hat{h}_{nu} \sim \mathcal{CN}\left(0, \frac{\rho_r \tau \beta_{nu}^2}{1 + \rho_r \tau \beta_{nu}}\right),$$

$$\hat{h}_{\text{nu}} \sim \mathcal{CN} \left(0, \beta_{\text{nu}} - \frac{\rho_r \tau \beta_{\text{nu}}^2}{1 + \rho_r \tau \beta_{\text{nu}}} \right),$$

Certainly! In the subsequent sections, we employ a composite methodology that integrates Principal Component Analysis (PCA) and the Least Mean Squares (LMS) algorithm. As delineated in Section I, this combined approach aims to enhance the performance of the system under study.

Principal Component Analysis

A dimensionality reduction method called Principal Component Analysis (PCA) may distinguish mixed signals in communication networks. It finds new vectors, called principal components, that have the most variation and independence in the data, PCA has many benefits for separating mixed signals in communication systems. First, PCA is easy and fast to implement in real-time systems. Second, PCA can handle noise and still separate the signals well even in noisy channels. Third, PCA can separate more than two signals, which makes it useful for many communication applications [25].

PCA is a dimensionality reduction technique that can enhance channel estimation in wireless communication systems. It projects the estimated channel data onto a lower-dimensional subspace that contains the most relevant information about the channel. This can lower the noise and interference in channel estimation, and boost the system performance, that can greatly improve the BER and MSE performance of channel estimation compared to LS estimation only. This is because PCA can lower the noise and interference in channel estimation, and increase the estimation accuracy [26]. PCA can compress data. It does this by finding a new set of basis vectors, called principal components that have the most variance in the data. These principal components are uncorrelated, which means they have independent information about the original data, by using only the most important principal components, PCA can achieve high compression ratios without losing much information. This is because the principal components with lower eigenvalues have the least relevance to the data, and can be discarded with minimal loss of fidelity [27].

Algorithm 1 divided mixed complex-valued signals into its component pieces using PCA. The real and imaginary components of a complex-valued matrix Z , represented as Z_{real} and Z_{imag} , respectively, are separated out of the matrix as input by the procedure. After computing the covariance matrices F_{real} and F_{imag} for the real and imaginary sections, Eigen decomposition is used to determine the eigenvalues and eigenvectors of each. The real and imaginary components of the input signals are projected independently onto the top n eigenvectors, which correspond to the greatest eigenvalues, which are chosen from both sets. Following projection, the real and imaginary components are combined to recreate the unique complex-valued signals. This synthesis furnishes a proficient method for the extraction of pertinent data from composite signals, which is instrumental for a multitude of signal processing applications.

PCA is widely used in signal processing applications. It finds a new set of vectors, called principal components that have the most variation in the data as shown in Figure 2. These principal components are independent of each other, which means they have independent information about the original signal, PCA can preserve most of the information in the signal by using only the most important principal components. This is possible because the principal components with the lowest eigenvalues have the least relevance to the signal, and can

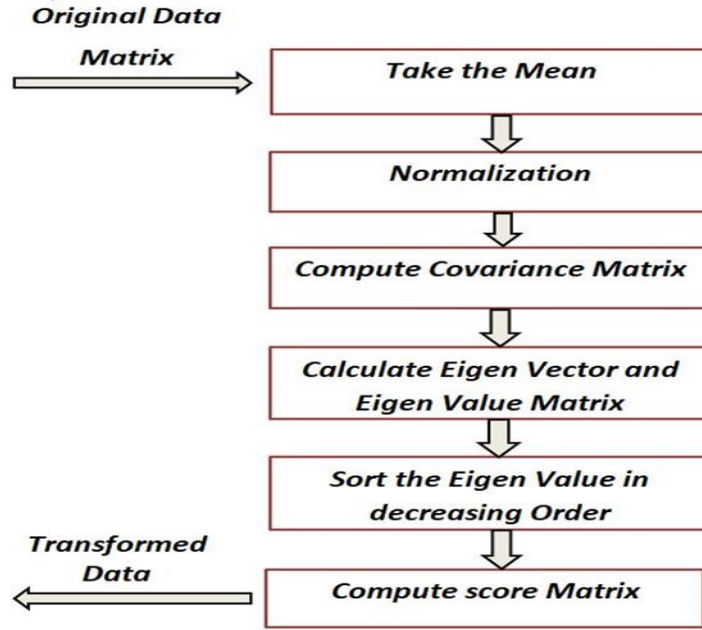


Figure 2: Flow chart for PCA Algorithm.

Algorithm 1 Principal Component Analysis (PCA) for separating shared pilot signals

Input: Complex-valued matrix $Z = [y_1 \ y_2 \ \dots \ y_n]$ representing the received mixed signals, where each column corresponds to a received signal, index for users that shared their pilot signals
 Output: target complex-valued signal (channel coefficient for user with shared pilot).

- 1: decouple the matrix Z into its real and imaginary parts
 - 2: $Z_{\text{real}} \leftarrow \text{Real}(Z)$
 - 3: $Z_{\text{imag}} \leftarrow \text{Imag}(Z)$
 - 4: calculate the covariance matrix F_{real} for the real part Z_{real}
 - 5: $F_{\text{real}} \leftarrow \text{Covariance}(Z_{\text{real}})$
 - 6: calculate the covariance matrix F_{imag} for the imaginary part Z_{imag}
 - 7: $F_{\text{imag}} \leftarrow \text{Covariance}(Z_{\text{imag}})$
 - 8: compute eigendecomposition on the F_{real} and F_{imag}
 - 9: $[V_{\text{real}}, O_{\text{real}}] \leftarrow \text{Eigendecomposition}(F_{\text{real}})$
 - 10: $[V_{\text{imag}}, O_{\text{imag}}] \leftarrow \text{Eigendecomposition}(F_{\text{imag}})$
 - 11: choose the top n eigenvectors related to the largest eigenvalues
 - 12: $V_{\text{real_top_n}} \leftarrow \text{Max Eigenvectors}(V_{\text{real}}, n)$
 - 13: $V_{\text{imag_top_n}} \leftarrow \text{Max Eigenvectors}(V_{\text{imag}}, n)$
 - 14: Do the projection on both real and imaginary on the PCA separately:
 - 15: $Z_{\text{real_projected}} \leftarrow V_{\text{real_top_n}}' \times Z_{\text{real}}$
 - 16: $Z_{\text{imag_projected}} \leftarrow V_{\text{imag_top_n}}' \times Z_{\text{imag}}$
 - 17: Combining both the real and imaginary signals projected to obtain the target signal
 - 18: The target signal $\leftarrow \text{Complex}(Z_{\text{real_projected}}, Z_{\text{imag_projected}})$
 - 19: end
-

Least Mean Square

Least Mean Square (LMS) is an adaptive filter algorithm that minimizes the MSE between the desired signal and the filter's output. It is simple, adaptive, and convergent, but it can also be slow, noisy, and ambiguous. LMS is widely used in signal processing applications, such as echo cancellation, noise cancellation, and channel equalization. It is a versatile and popular algorithm, but it has some limitations [28] [29]. Using the LMS algorithm, an adaptive technique, the channel response at pilot frequencies is estimated in wireless systems with comb-type pilot arrangement, where pilot signals are evenly distributed among the data subcarriers. Figure 3 shows the flow chart of LMS algorithm where a one-tap adaptive filter is applied at each pilot frequency. The LS method gives the initial channel estimate at pilot frequencies, and later estimates are based on the earlier estimation and the current channel output. The LMS algorithm reduces the mean square error between the pilot signals that were sent and received by updating the channel estimate iteratively, The LMS algorithm is a computationally efficient and adaptive method for channel estimation in wireless communication systems with dynamic channels. It can better capture the variations in the channel response than block-based estimation methods [30] [29]. The LMS algorithm is a widely used adaptive filter technique introduced by Widrow. We applied algorithm 2 to minimize the mean square error between the desired signal and the estimated signal obtained from algorithm 1. The algorithm 2 adjusts the filter weights continuously to achieve this goal, in the algorithm, the filter output is a linear combination of input samples. The discrepancy between the intended output and the filter output is the error. The algorithm is computationally efficient and only needs about $2 * L$ multiplications per iteration, where L is the filter length. However, it only gives an approximate solution for the optimal weights, with weight updates based on imperfect gradient estimates.

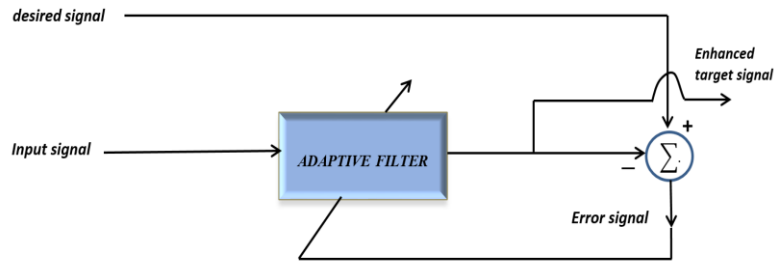


Figure 3: Flow chart for LMS Algorithm.

Algorithm 2 Least Mean Square (LMS)

Input: Initial estimate of the channel coefficient obtained from algorithm 1, desired pilot signal, step size μ , and iterations number.

Output: Enhanced target signal

1. Initialize: set the input signal = Output of algorithm 1
2. **for** iteration = 1 to iterations number **do**
3. Calculate the error signal $e = \text{desired pilot signal} - \text{enhanced target signal}$
4. Update the enhanced signal

$$\text{Enhanced target signal} = \text{input signal} + \mu * e.$$

5. **end for**

Numerical Results

We investigate a 2×2 km² densely populated region with wrap-around (to avoid border impacts). It is also assumed that N APs and U users are dispersed randomly. We use the COST_Hata model for coefficients large-scale fading

$$10 \log_{10} \beta_{nu} = -136 - 35 \log_{10}(d_{nu}) + Z_{nu} \quad (4)$$

Where d_{nu} is the distance between antenna, n and user, u in kilometres and $Z_{nu} \sim \mathcal{N}(0, \sigma_{shad}^2)$ with $\sigma_{shad} = 8$. The receiver noise variance is $\sigma_s^2 = 290 \times \mathcal{K} \times \mathcal{B} \times \mathcal{NF}$, where \mathcal{B} , \mathcal{K} and \mathcal{NF} are bandwidth (20MHz), Boltzmann constant and noise figure (9 dB) respectively.

TABLE I: Simulation Parameters

Parameters	Values
Standard deviation shadowing	8 dB
Power transmitted by every U	20 dBm
AP radiated power	30 dBm
frequency of carriers	1.9 GHz
The bandwidth	20 MHz
Noise figure	9 dB
Thermal noise level	- 174 dB m\Hz
Height of the AP antenna	15 m
Height of the U antenna	1.65 m
d_1	50 m
d_0	10 m
N	128
U	8

We conduct a simulation with $N = 128$ and $U = 8$. The operation of the system was executed in alignment with the procedural schematic delineated in Figure 4. To assess the average channel estimation performance of orthogonal pilot sequences. Subsequently, this was compared to the channel condition performance resulting from pilot assignment as documented in reference [16] as well as to the outcomes derived from processing utilizing our suggested algorithms.

The relationship between normalized mean squared error (NMSE) of the Cell-Free Massive MIMO systems and the signal to noise ratio (SNR) is depicted in figure 5 where the horizontal axis denotes the SNR and the vertical axis represents the NMSE. We observe that the NMSE value decreases as the SNR value increases, and this decrease implies better accuracy in signal reception.

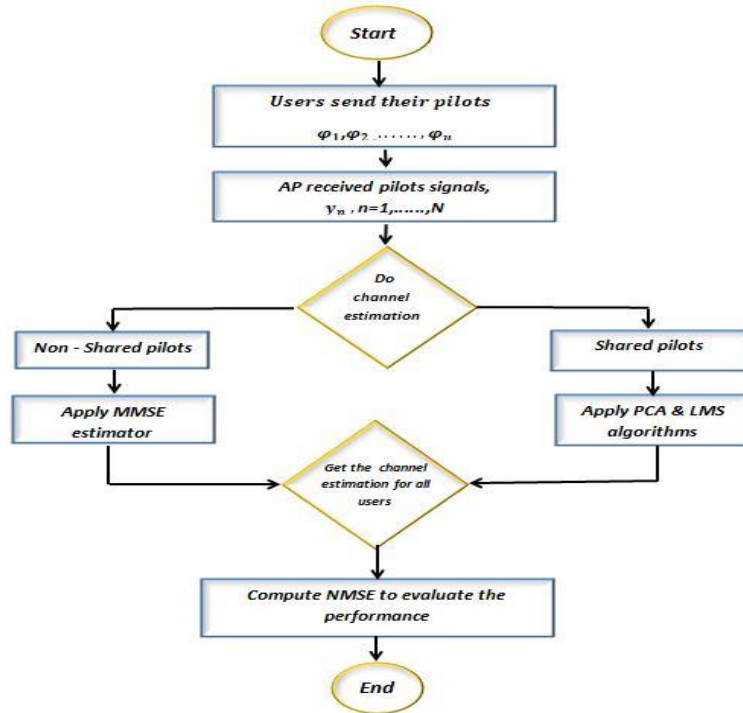


Figure 4: Flow chart for System Model

For instance, at SNR = 10 dB, that $NMSE = 12.39 \times 10^{-3}$ for pilot assignment as documented in reference [16] and this is the worst performance, while $NMSE = 3.229 \times 10^{-4}$ for orthogonal pilot sequences and this is the best performance, but also comparable to the performance of the proposed algorithm, which $NMSE = 4.318 \times 10^{-4}$ also this is the better performance compared with the non-orthogonal without any processing. We note that when SNR is low, the performance of the algorithm, whether it is orthogonal or pilot assignment referenced in [16], or the proposed algorithm, is worse due to the high noise level and therefore the proposed algorithm benefits from the increase of SNR.

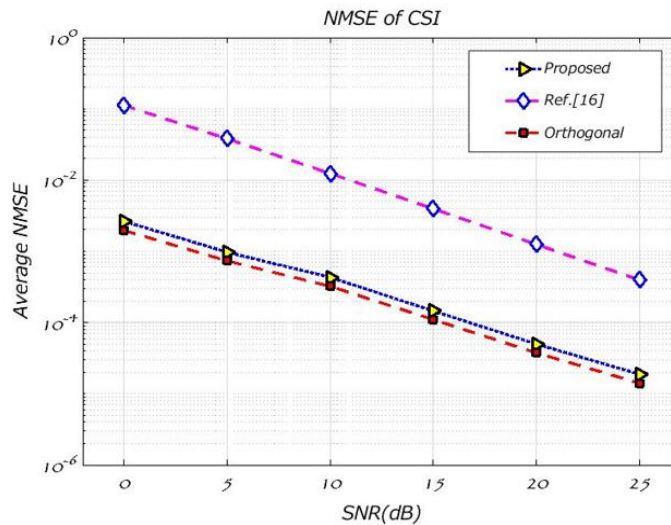


Figure 5: Average NMSE against SNR, Here, N = 128, U = 8

In figure 6, the horizontal axis represents number of antennas at the access point (AP) and the vertical axis represents normalized mean square error (NMSE). The figure depicts the relationship between

the NMSE of a cell-free massive MIMO system and the number of antennas at the AP. We observe that the NMSE value decreases as the antenna count at the AP rises, and this decrease implies better accuracy in signal reception.

For instance, at No .of antenna (AP) = 128, the NMSE = 12.29×10^{-3} for pilot assignment as documented in reference[16], and this is the worst performance, while NMSE = 3.192×10^{-4} for orthogonal experimental sequences and this is the best performance. However, our proposed algorithm significantly improves the NMSE which yields NMSE = 4.252×10^{-4} and shows comparable performance to the orthogonal pilots.

We note that when the number of antennas at the AP is low, the performance of the algorithm, whether it is orthogonal or pilot assignment referenced in [16], is worse due to the limited number of antennas at the AP and therefore the proposed algorithm benefits from increasing the number of antennas at the AP.

Hence, the number of antennas at the AP has a significant impact on the accuracy of signal reception.

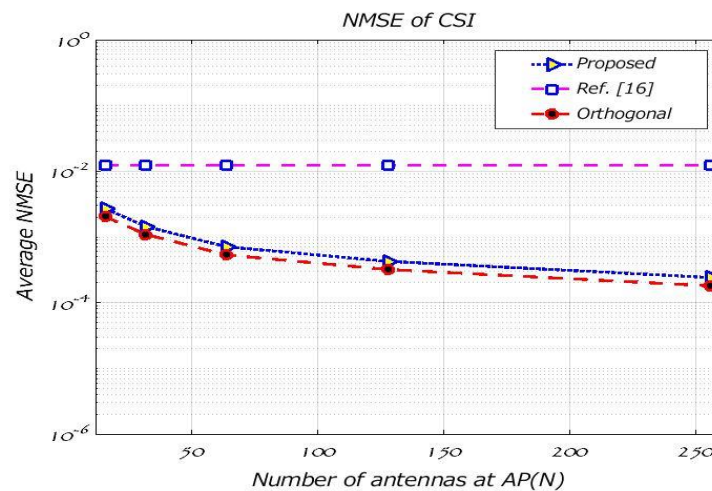


Figure 6: Average NMSE against Number of antenna at (AP), Here, N = 128, U= 8.

In contrast, we will assess the system's functionality in the event that the user base grows or shrinks, Figure 7 explores the relationship between the Normalized Mean Squared Error (NMSE) of a cell free massive MIMO system and the number of users. The horizontal axis represents the number of users, while the vertical axis represents the NMSE. We observe a decreasing trend in NMSE as the number of users increases, indicating improved signal reception accuracy with a larger user base. For instance, at U= 20 users , the NMSE for pilot assignment as documented in Reference [16] is 4.984×10^{-3} , representing the worst performance . In contrast, orthogonal experimental sequences achieve the best performance with an NMSE of 9.065×10^{-5} . Notably, our proposed algorithm significantly improves the NMSE, yielding a value of 1.769×10^{-4} and demonstrating comparable performance to orthogonal pilots.

However, it is important to acknowledge that when the number of users is low, the performance of all algorithms (orthogonal, pilot assignment from [16], and the proposed method) is worse. This is likely due to the high user density, which can lead to increased interference. Interestingly, the proposed algorithm benefits from a larger user base, suggesting its potential for efficient operation in dense user scenarios.

While increasing the number of users can enhance system capacity and spatial diversity, it is crucial to employ careful design and resource management techniques to maintain overall performance. Advanced approaches like beamforming, interference cancellation, and user grouping can further

improve system performance even with a large number of users. Ultimately, striking a balance between the number of users and resource management strategies is essential for achieving optimal results.

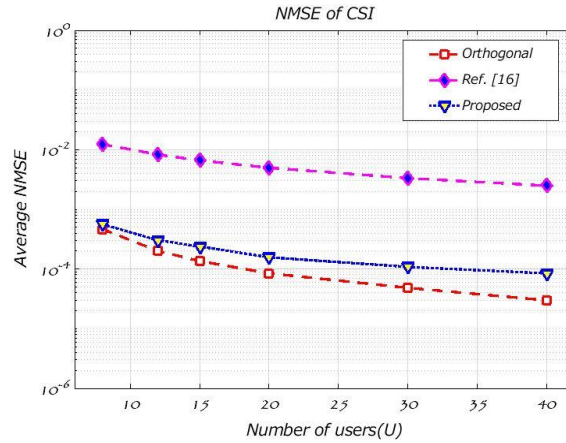


Figure 7: Average NMSE against Number of Users (U), Here, N = 128, U= 8,10,15,20,25,30,35 and 40.

The relationship between the NMSE of the cell free massive MIMO systems and the length of training (τ) is depicted in figure 8 where the horizontal axis represents the length of training (τ) and the vertical axis represents the mean normalized square error (NMSE). We observe that the NMSE value decreases as the length of training (τ) increases, and this decrease implies better accuracy in signal reception.

For instance, when no. of length of training (τ) = 30, the NMSE = 3.311×10^{-3} for pilot assignment as documented in reference[16], and this is the worst performance, while the NMSE = 1.099×10^{-4} for orthogonal pilots and this is the best performance. However, our proposed algorithm significantly improves the NMSE which yields NMSE = 1.475×10^{-4} and shows comparable performance to the orthogonal pilots.

We note that the length of training is a measure of the duration of the signal processing algorithm during training phase. The length of training leads to an increase in processing time, and therefore the longer the length of training, the better the system performance.

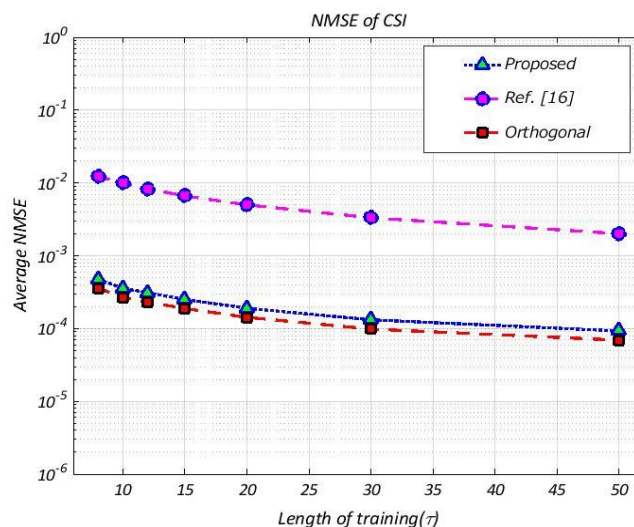


Figure 8: Average NMSE against Length of Training (τ), Here, N = 128, U= 8.

CONCLUSION

In traditional cell-free massive MIMO systems, the deployment of unique orthogonal pilot sequences by users necessitates the availability of an extensive array of such sequences. In scenarios where the pilot sequences are limited, Pilot Contamination becomes a concern, resulting in user interference due to the utilization of shared sequences. To surmount this obstacle and improve channel quality estimation, a hybrid methodology combining Principal Component Analysis (PCA) and the Least Mean Squares (LMS) algorithm was employed for the segregation of users within the ambit of shared pilot sequences. The method introduced in this study exhibited a substantial improvement in performance when compared to the traditional pilot assignment approach. The integrated PCA-LMS strategy revealed significant enhancements in system efficiency over the individual methods. Furthermore, the proposed method demonstrated an exceptional elevation in the overall performance of the system.

REFERENCES

- [1] H. Q. Ngo, A. Ashikhmin, H. Yang, E. G. Larsson, and T. L. Marzetta, "Cell-free massive MIMO versus small cells," *IEEE Trans. Wirel. Commun.*, vol. 16, no. 3, pp. 1834–1850, 2017.
- [2] S. Buzzi and C. D'Andrea, "Cell-Free Massive MIMO: User-Centric Approach," *IEEE Wirel. Commun. Lett.*, vol. 6, no. 6, pp. 706–709, 2017, doi: 10.1109/LWC.2017.2734893.
- [3] A. A. I. Ibrahim, A. Ashikhmin, T. L. Marzetta, and D. J. Love, "Cell-free massive MIMO systems utilizing multi-antenna access points," in *2017 51st Asilomar Conference on Signals, Systems, and Computers*, 2017, pp. 1517–1521.
- [4] J. Zhang, Y. Wei, E. Björnson, Y. Han, and X. Li, "Spectral and energy efficiency of cell-free massive MIMO systems with hardware impairments," in *2017 9th International Conference on Wireless Communications and Signal Processing (WCSP)*, 2017, pp. 1–6.
- [5] H. Yang and T. L. Marzetta, "A macro cellular wireless network with uniformly high user throughputs," in *2014 IEEE 80th vehicular technology conference (VTC2014-Fall)*, 2014, pp. 1–5.
- [6] T. C. Mai, H. Q. Ngo, and T. Q. Duong, "Uplink spectral efficiency of cell-free massive MIMO with multi-antenna users," in *2019 3rd International Conference on Recent Advances in Signal Processing, Telecommunications & Computing (SigTelCom)*, 2019, pp. 126–129.
- [7] E. Nayebi, A. Ashikhmin, T. L. Marzetta, and B. D. Rao, "Performance of cell-free massive MIMO systems with MMSE and LSFD receivers," in *2016 50th Asilomar Conference on Signals, Systems and Computers*, 2016, pp. 203–207.
- [8] H. Almosa, Y. J. Harbi, M. Al-Dulaimi, and A. Burr, "Performance Analysis of DoA Estimation for FDD Cell Free Systems Based on Compressive Sensing Technique," *J. Commun.*, vol. 18, no. 10, pp. 658–664, 2023.
- [9] D. C. Araújo, T. Maksymyuk, A. L. F. de Almeida, T. Maciel, J. C. M. Mota, and M. Jo, "Massive MIMO: survey and future research topics," *Iet Commun.*, vol. 10, no. 15, pp. 1938–1946, 2016.
- [10] S. Mosleh, H. Almosa, E. Perrins, and L. Liu, "Downlink resource allocation in cell-free massive MIMO systems," in *2019 International Conference on Computing, Networking and Communications (ICNC)*, 2019, pp. 883–887.
- [11] Z. Chen and E. Björnson, "Can we rely on channel hardening in cell-free massive MIMO?," in *2017 IEEE Globecom Workshops (GC Wkshps)*, 2017, pp. 1–6.
- [12] E. Nayebi, A. Ashikhmin, T. L. Marzetta, H. Yang, and B. D. Rao, "Precoding and power optimization in cell-free massive MIMO systems," *IEEE Trans. Wirel. Commun.*, vol. 16, no. 7, pp. 4445–4459, 2017.
- [13] T. C. Mai, H. Q. Ngo, M. Egan, and T. Q. Duong, "Pilot power control for cell-free massive MIMO," *IEEE Trans. Veh. Technol.*, vol. 67, no. 11, pp. 11264–11268, 2018.
- [14] X. Zhu, Z. Wang, L. Dai, and C. Qian, "Smart pilot assignment for massive MIMO," *IEEE Commun. Lett.*, vol. 19, no. 9, pp. 1644–1647, 2015.

- [15] E. Nayebi, A. Ashikhmin, T. L. Marzetta, and H. Yang, "Cell-free massive MIMO systems," in 2015 49th Asilomar Conference on Signals, Systems and Computers, 2015, pp. 695–699.
- [16] E. Björnson and L. Sanguinetti, "Scalable cell-free massive MIMO systems," *IEEE Trans. Commun.*, vol. 68, no. 7, pp. 4247–4261, 2020.
- [17] H. Wang, D. Yang, X. Li, and P. Pan, "How Many Signals Can Be Sent in a Multi-Cell Massive MIMO System," *IEEE Wirel. Commun. Lett.*, vol. 7, no. 3, pp. 368–371, 2017.
- [18] G. Interdonato, E. Björnson, H. Quoc Ngo, P. Frenger, and E. G. Larsson, "Ubiquitous cell-free massive MIMO communications," *EURASIP J. Wirel. Commun. Netw.*, vol. 2019, no. 1, pp. 1–13, 2019.
- [19] T. L. Marzetta, "Noncooperative cellular wireless with unlimited numbers of base station antennas," *IEEE Trans. Wirel. Commun.*, vol. 9, no. 11, pp. 3590–3600, 2010.
- [20] N. Akbar, S. Yan, N. Yang, and J. Yuan, "Location-aware pilot allocation in multicell multiuser massive MIMO networks," *IEEE Trans. Veh. Technol.*, vol. 67, no. 8, pp. 7774–7778, 2018.
- [21] M. Bashar, K. Cumanan, A. G. Burr, H. Q. Ngo, and M. Debbah, "Cell-free massive MIMO with limited backhaul," in 2018 IEEE International Conference on Communications (ICC), 2018, pp. 1–7.
- [22] H. Q. Ngo, L.-N. Tran, T. Q. Duong, M. Matthaiou, and E. G. Larsson, "On the total energy efficiency of cell-free massive MIMO," *IEEE Trans. Green Commun. Netw.*, vol. 2, no. 1, pp. 25–39, 2017.
- [23] S. Rao, A. Ashikhmin, and H. Yang, "Cell-free massive MIMO with nonorthogonal pilots for Internet of Things," *arXiv Prepr. arXiv2006.10363*, 2020.
- [24] Y. KAKISHIMA, "Non-Orthogonal Pilot Designs for Joint Channel Estimation and Collision Detection in Grant-Free Access Systems".
- [25] J. Ma and X. Zhang, "Blind source separation algorithm based on maximum signal noise ratio," in 2008 First International Conference on Intelligent Networks and Intelligent Systems, 2008, pp. 625–628.
- [26] M. Nasserri, H. Bakhshi, S. Sahebdel, R. Falahian, and M. Ahmadi, "PCA Application in Channel Estimation in MIMO-OFDM System," *Int. J. Commun. Netw. Syst. Sci.*, 2011.
- [27] A. P. Ferreira and M. Toba, "Multivariate analysis in the pharmaceutical industry: enabling process understanding and improvement in the PAT and QbD era," *Pharm. Dev. Technol.*, vol. 20, no. 5, pp. 513–527, 2015.
- [28] S. Haykin and B. Widrow, "Least-Mean-Square Adaptive Filters," 2003.
- [29] Y. Chen, Y. Gu, and A. O. Hero, "Sparse LMS for system identification," in 2009 IEEE International Conference on Acoustics, Speech and Signal Processing, 2009, pp. 3125–3128.
- [30] S. Colieri, M. Ergen, A. Puri, and A. Bahai, "A study of channel estimation in OFDM systems," in Proceedings IEEE 56th vehicular technology conference, 2002, vol. 2, pp. 894–898.